Assessment of Conceptual Noise Reduction Devices for A Main Landing Gear using SNGR Method

Hua-Dong Yao[1*] , Lars Davidson[1†]

Shia-Hui Peng[1,2‡]

Francesco Capizzano[3§] , Mattia Barbarino[3¶] , Giuseppe Mingione[3‖]

1. Chalmers University of Technology, SE-412 96 Gothenburg, Sweden

2. Swedish Defence Research Agency (FOI), SE-164 90 Stockholm, Sweden

3. C.I.R.A., Italian Aerospace Research Center, 81043 Capua (CE), Italy

The noise-reduction efficiencies of three conceptual designs are explored for a main landing gear (MLG) mounted on a simplified fuselage body with a bay and gear door. The designs are a fairing attached on the strut, compression of the bay space as the gear is deployed, and acoustic liners installed in the interior downstream wall of the bay. The gear door is opened in order to investigate its reflection effect on the noise during the operation. The stochastic noise generation and radiation (SNGR) method coupled with the Reynolds-averaged Navier-Stokes (RANS) equations are used for the noise prediction. This approach has the advantage to speed up the computation of both the fluid flow and noise. The Cartesian immersed boundary method (IBM) that is employed for the RANS solver further shortens the period of the overall assessment process due to fast and automatic mesh generation. The present SNGR method integrates the Lighthill analogy and the boundary element method (BEM). The Lighthill analogy is used for the prediction of the noise produced by a synthetic turbulent field that is constructed with a stochastic model based on the time-averaged turbulence quantities obtained from the RANS solution. The BEM is applied to compute the surface-scattered noise. The current fairing design is found

---

*Division of Fluid Dynamics, Department of Applied Mechanics, huadong@chalmers.se

†Division of Fluid Dynamics, Department of Applied Mechanics, lada@chalmers.se

‡Division of Fluid Dynamics, Department of Aeronautics and Systems Technology, shia-hui.peng@foi.se

§f.capizzano@cira.it

¶m.barbarino@cira.it

‖g.mingione@cira.it

American Institute of Aeronautics and Astronautics

inefficient for the noise reduction. The strategy of reducing the bay depth is not functional as well. However, the liners are effective for absorption of the acoustic pressure on the surfaces. Moreover, the noise reflection effect of the gear door is clarified. Since the horizontally projected area of the door is not negligible, the noise reflected towards the ground is found significant in the high frequency range. The conclusion is that a gear door and the way of arranging it in the gear-deployed stage should be regarded as the important factors of the product design.

I. Introduction

One of the dominant sources of airframe noise is the turbulence induced by landing gears.[1] The strategies and devices designed for reducing the noise have raised intensive interests in industry.[2] A conceptual design in general is expected to control the turbulence or to absorb the noise reflected by surfaces. The expectation can be fulfilled by mounting additional devices or by optimizing the aerodynamic geometries of struts, axles and bays and so on.

An add-on facility for depressing the turbulence is a fairing shielding a landing gear. Dobrzynski et al.[3–6] investigated rigid fairings that prevented the flow interaction between a strut and bay (often called cavity). The fairings were found with the noise-reduction benefit, but they were possible to form the new noise sources. Piet et al.[7] put forward and explored a set of perforated fairings. Their research, which included both measurements and numerical simulations, proved the effectiveness of the perforated fairings, even though a slight drag increase appeared due to these add-on elements. Furthermore, various strategies on the fairing construction have been proposed and examined.[8–11] In a recent work conducted by Murayama,[12] a rigid faring and a porous fairing were compared for the same landing gear based on the results of steady RANS computations.

The surface-reflected noise can be attenuated by mounting acoustic liners on structure surfaces. This treatment for engine internal walls has been widely recognized efficient to reduce the engine noise.[13–15] Another application of the acoustic liners have been explored for damping trailing edge noise.[16–19] The application indicates that the acoustic liners possess the potential to damp other types of the airframe noise.

In a real flight operation, the gear door is opened as a gear is deployed. Lopes[20] assessed the influence of a gear door on the noise generation. It was found that the door depressed the turbulent shedding induced by the oleo leg and therefore reduced the noise. Moreover, the normal direction of the door was arranged approximately parallel to the ground so that the horizontally projected area of the door is negligible. The arrangement makes the door reflect a low portion of the noise towards the ground. However, in the situation that the horizontally-projected area of a deployed door is discernible, the reflected noise is not clearly

American Institute of Aeronautics and Astronautics

investigated.

To down select efficient low-noise designs, numerical simulations are regarded as fast and cheap means. However, the composite structures of landing gears challenges the techniques for both the computational fluid dynamics (CFD) and computational aero-acoustics (CAA). An obvious problem is that the computational costs and memory requirement dramatically increase due to refined body-fitted grids that are used for the CFD or CAA computation. A cheap approach of simulating turbulence is to solve the Reynolds-averaged Navier-Stokes (RANS) equations. However, this approach cannot provide the time-dependent information of the turbulent fluctuations that are necessary for the prediction of the noise. To solve this deficiency of RANS, the stochastic noise generation and radiation (SNGR) method was proposed.[21, 22] It has been applied to a number of industrial applications.[23–25] The SNGR method in general integrates two steps, i.e., the construction and formulation of the noise sources, and the propagation of the noise. On the basis of the statistics obtained from the RANS solution, the stochastic model[26] is utilized to construct a synthetic turbulent field, in which the velocity fluctuations are regarded as the noise sources. The mathematical forms of the sources are then formulated according to the CAA approaches like the linearized Euler equations (LEE) [24] or acoustic analogies.[27, 28] Correspondingly, the noise propagation is computed by solving the LEE or the wave propagation equation.

This work aims at addressing three noise-reduction concepts for a main landing gear (MLG). Moreover, since the gear door should be opened in the operation situation, its reflection effect to the noise will be explored. The present SNGR method coupled with RANS will be examined as an efficient numerical approach for prediction of the MLG noise. The noise generation and radiation are resolved with the Lighthill acoustic analogy[27, 28] and boundary element method (BEM).[29] An in-house code of the immersed boundary (IB) method will be taken for the RANS computation due to the low cost for the mesh generation.[30]

II.   Conceptual Noise-Reduction Designs

The MLG configuration investigated is full-sized and operates at the flight Reynolds number. The gear door is opened in order to make clear its contribution on the reflected noise. Figure 1 shows the baseline configuration. The green plane is the symmetric plane of the geometry. The MLG is mounted on a simplified fuselage that is of streamwise length approximately 10.6 times the wheel diameter D_{wh}.

Figure 2 illustrates the noise-reduction strategies and devices in comparison with the baseline configuration. The red color highlights these designs. The fairing is partially merged into the strut. Alternatively, the depth of the bay is reduced by extruding a plate in the bay when the MLG is deployed. The third concept is to patch the acoustic liners in the bay interior downstream wall, which is not shown here. The baseline
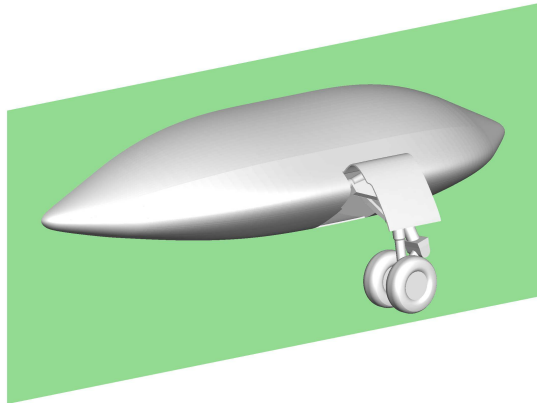
Figure 1. The baseline configuration. The symmetric plane of the configuration is shown in green.

MLG configuration and noise-reduction designs are listed in Table 1.
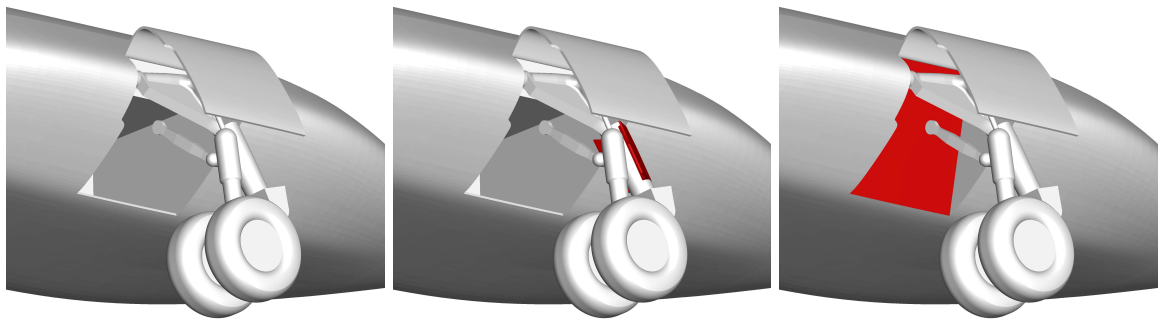

Figure 2. (a) The baseline configuration, (b) the baseline configuration with the fairing and (c) with the reduced bay depth. The red color marks the modified elements with respect to the baseline. The freestream flow goes from right to left.

The configurations operate with the angle of attack $\alpha = 0^o$. By assigning this attack angle deliberately, the deployed gear door will not introduce strong turbulent shedding, which can be a new potent noise source. Moreover, the reflected noise can be focused if other noise related to the door is eliminated. The flight Reynolds number Re_∞ is 4.75×10^6 per meter, and the Mach number M_∞ is 0.204. The ambient pressure p_∞ is $1.01325 \times 10^5 Pa$, and the ambient density $\rho_\infty = 1.225 kg/m^3$.

American Institute of Aeronautics and Astronautics

Table 1. The noise-reduction conceptual designs for the MLG configuration[†]

	Low-noise concepts
Config. 1	The baseline
Config. 2	a fairing merged in the strut
Config. 3	Reduction of the bay depth
Config. 4	Acoustic liners installed the bay downstream interior wall

† The door of the MLG bay is opened.

III.   Numerical Methodologies

A.   CFD method for Aerodynamic Simulations

An IB technique has been developed at CIRA, which is based on automatic generation of locally refined Cartesian meshes.[31] Experiences was matured in wall modelling for compressible two- and three-dimensional high Reynolds number flows mainly during the activities of the JTI-GRA and JTI-GRC European projects. A fully unstructured data management is adopted to deal with Cartesian meshes.[32]

A cell-centered finite volume method is used to solve the RANS equations for compressible flow. The convective and diffusive fluxes are approximated by using a central difference scheme (CDS), which is 2nd order accurate in space. The amount of added artificial diffusion is controlled in each cell by a matrix linked to the Jacobian of convective fluxes (matrix artificial diffusion MATD). A three stage explicit Runge-Kutta pseudo-time integration is carried out to find a steady state solution for the RANS and the turbulence model equations which are solved simultaneously. The $k - \omega$ TNT turbulence model is utilized. The basic scheme is modified near the wall by means of an IB approach. It includes a discrete forcing in the momentum equation in the way of a direct BC imposition. Proper fluxes are introduced at the near-wall cells to satisfy the Dirichlet/Neumann conditions on the wall. A turbulent wall model is used to reconstruct nonlinear quantities at high Reynolds numbers.[30] The numerical schemes and algorithms are optimized to run on vectorial and parallel architectures to make affordable three-dimensional numerical experiments.

B.   SNGR Method for Acoustic Computations

The SNGR method is fast and simple, since the turbulence is synthesized using the stochastic model.[26, 33] The time-averaged information of the field required by the stochastic model comes from a RANS computation. The time-averaged kinetic energy and dissipation rate are the variables needed for the construction of the synthetic turbulent field. These velocity fluctuations are transformed to the noise source terms based on the

Lighthill analogy.[27, 28] The Lighthill equation is then used to generate the noise in free space and propagate it onto the surrounding surfaces. The noise scattered by the surfaces is computed using the BEM.[29] The overall acoustic computation is undertaken in frequency space.

Since FINE/Acoustics[TM] produced by NUMECA includes the tool of the SNGR method described above, it is the preferable choice for the present work. The details of the SNGR method refer to the user manual of FINE/Acoustics[TM], as well as another paper of the authors.[34]

IV. Computational Settings

A. RANS Solutions of Turbulent Flow

The configurations are placed a computational domain that the origin of the Cartesian coordinate system is located at the apex of the nose of the simplified fuselage. The domain is specified with $-100 \leq x/D_{wh} \leq 200$ in the freestream flow direction aligned with the X-axis, $0 \leq y/D_{wh} \leq 50$ in span, and $-100 \leq z/D_{wh} \leq 100$ in vertical direction.

A Cartesian uniform mesh, which have a root cell dimension of $\Delta_{far-field} = 2D_{wh}$, is recursively refined near the wall to obtain a near-wall minimum spacing of $\Delta_{wall} = 0.008D_{wh}$ after 8 refinement levels. The buffer layers of uniform cells are forced inside the boundary layer. The meshes are separately generated for the configurations in terms of the same quality criteria. The CFD mesh generated for the baseline configuration is illustrated in Fig. 3.
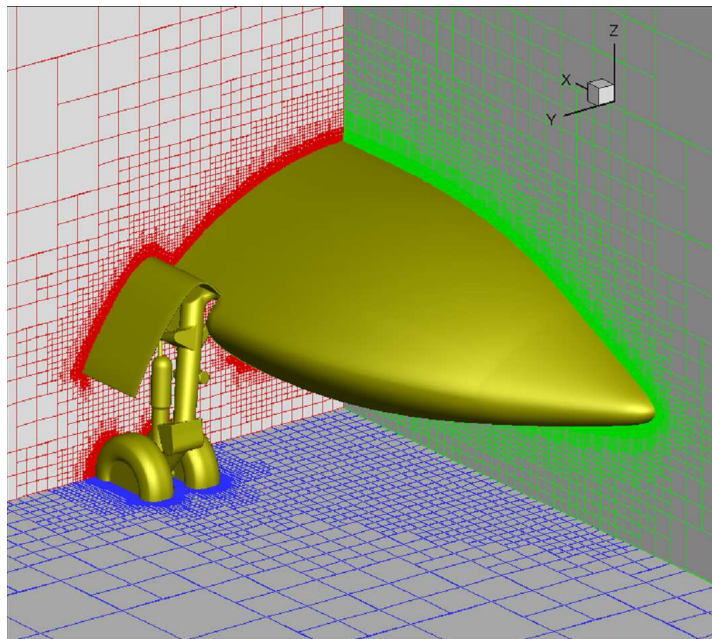

Figure 3. The CFD mesh generated for the baseline configuration.

American Institute of Aeronautics and Astronautics

The inlet is set in the plane of $x = -100D_{wh}$, and the outlet in the plane of $x = 200D_{wh}$. The classical inflow and outflow boundary conditions based on characteristic conditions are imposed at the inlet and outlet, respectively. The symmetric boundary condition is imposed on the symmetric plane of the domain, $y = 0$, to save computational costs. The rest of the lateral boundaries are set with the far-field boundary condition. The non-slip boundary condition is enforced on the geometry surfaces via the ad-hoc IB wall-modelling developed by Capizzano.[30]

The acoustic liners are assumed to have negligible impact on the flow. Hence, the RANS solution for the baseline configuration is directly adopted for Configuration 4 with the acoustic liners.

B.   Settings for Acoustic Field

Since the flow field is solved using the IB Method, the CFD mesh is not aligned with the walls. If the nodes inside the object are not treated in a proper way, they will be regarded as the noise sources located within the object. These unphysical noise sources will bring the numerical contamination for the acoustic computation. Moreover, it is known that the accuracy of the BEM would be best preserved with a homogeneous mesh. Therefore, an CAA mesh is required to remove the unphysical noise sources and to improve the inhomogeneous node distribution. The RANS solution with the original CFD mesh is interpolated to this CAA mesh.

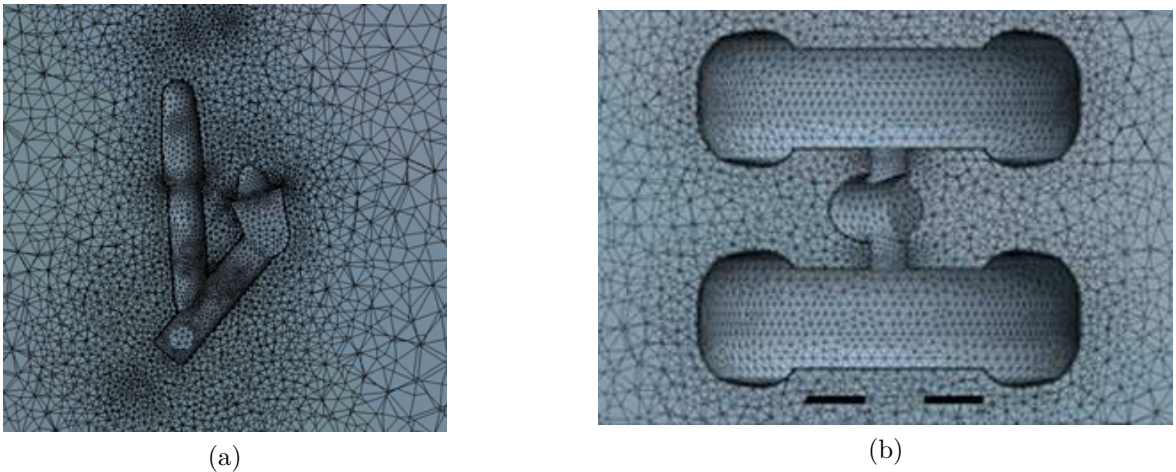(a)   (b)

Figure 4. The volume elements of the CAA mesh generated for the baseline configuration.

The size of the volume elements of the CAA mesh is set to below $\Delta_{max} = 0.05D_{wh}$. The height of the first layer adjacent to the walls is $0.001D_{wh}$. There are four mesh layers to resolve the boundary layer. Figure 4 shows the volume elements around the strut and wheels for the CAA mesh of the baseline configuration. The surface grids are nearly homogeneous. The maximum size of the surface elements is $0.03D_{wh}$. The surface

elements on the interior walls of the bay and on the wheels are displayed for the CAA mesh of the baseline configuration in Fig. 5.
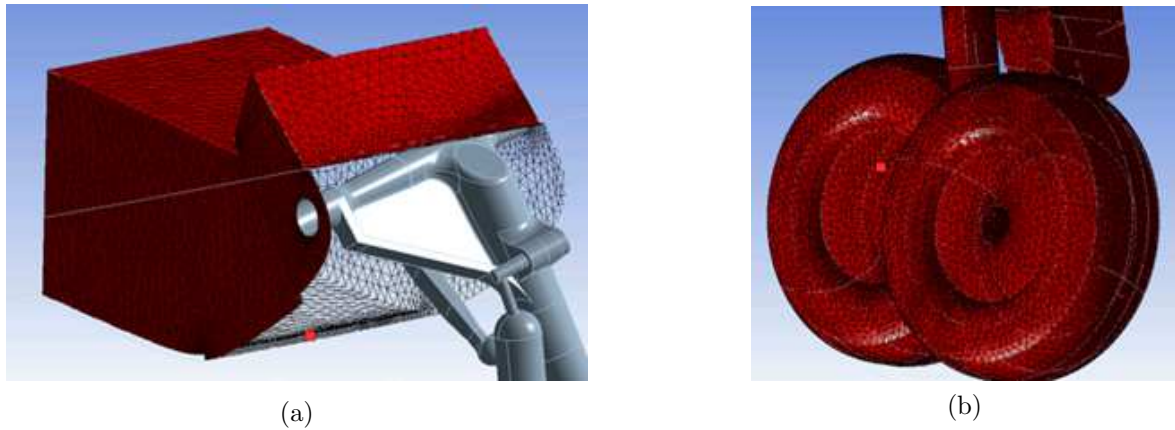

(a)　　　　　　　　　　　　　　　　　　　　(b)

Figure 5.　The surface elements of the CAA mesh generated for the baseline configuration.

The major noise sources are assumed to be located in the region where the normalized time-averaged turbulent kinetic energy, $\overline{k}_e = k_e/U_\infty^2$, is higher than 2.08×10^{-4}. Figure 6 shows the iso-surface for $\overline{k}_e$ of this magnitude. The colors on the iso-surface represent specific dissipation rate ω. Subfigure (c) in the left column shows that the fairing causes an extensive wake. The fairing results in lower specific dissipation on the front side of the strut than the baseline configuration. However, the specific dissipation becomes high on the back side of the strut. The fairing induces more noise sources near the bay mouth. The configuration with the reduced bay depth brings about more downstream noise sources close to the fuselage compared with the others, as displayed in the subfigures in the right column. It indicates that the reduced bay leads to strong flow interaction between the strut and bay mouth.

The locations of the microphones are illustrated in Fig. 7. The placement of microphone array is specified in a polar arc (between 20° and 160°) beneath the MLG with distance $30m$. The interval angle between the microphones is 10°. The origin of the microphone arc is positioned at the center of the gear door.
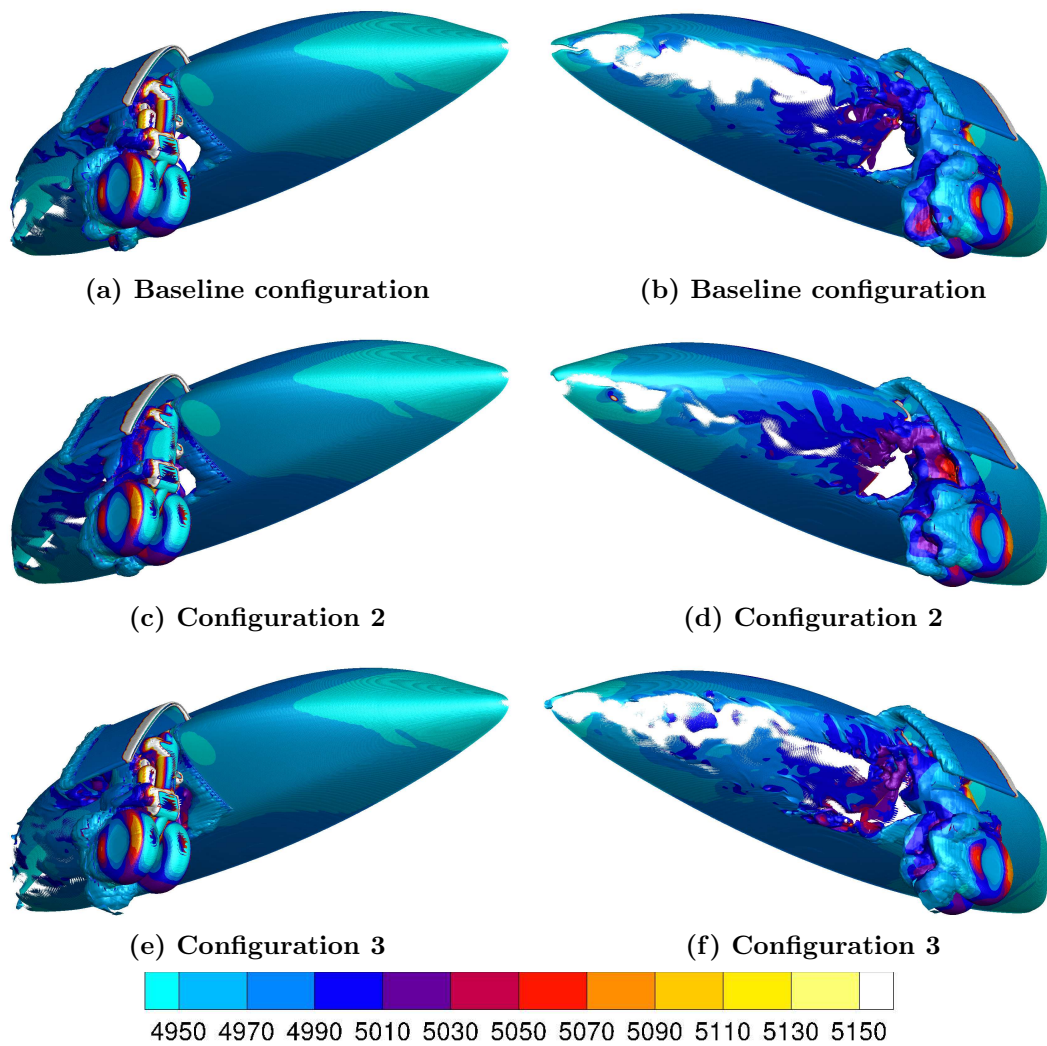
American Institute of Aeronautics and Astronautics

(a) Baseline configuration   **(b) Baseline configuration**

(c) Configuration 2   **(d) Configuration 2**

(e) Configuration 3   **(f) Configuration 3**

4950 4970 4990 5010 5030 5050 5070 5090 5110 5130 5150

Figure 6. **The isosurface of $\overline{k} = 2.08 \times 10^{-4}$. The color displays ω. The left and right columns show the configurations in the front and back views, respectively.**

Flow direction
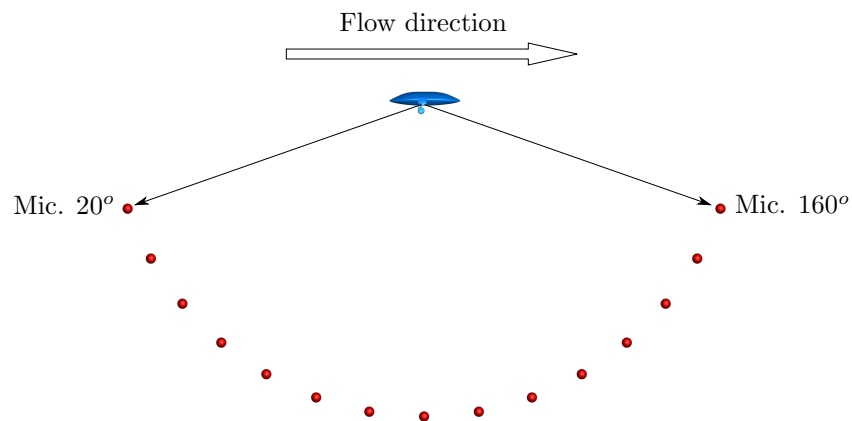
Mic. 20° Mic. 160°

Figure 7. The placement of the microphone array.

V.   Results and Discussion

Overall sound pressure level of A-weighted scale (OASPLA) for the noise in the microphone array is plotted in Fig. 8. The upstream of the MLG is set towards 0°. The microphone at 90° faces the opened gear door. However, the noise level at the microphone, 100°, is higher than those at the other microphones. This microphone relates to the location of the wake that is induced by the wheels and strut. The turbulent wake forms only quadrupole sources that emit the noise with approximately even energy distribution in all directions, whereas the noise reflected by surfaces propagates with a clear dipole directivity. In addition, the trailing edge noise induced by the door is negligible since the angle of attack is 0°. Therefore, the high noise level at 100° indicates that the door reflects the noise from the turbulent wake. The averaged OASPLA that accounts for all the microphones is compared between the baseline configuration and the noise-reduction concepts in Table 2. The acoustic liners (Configuration 4) reduce the noise by $1.8 dBA$ in reference to the baseline case.
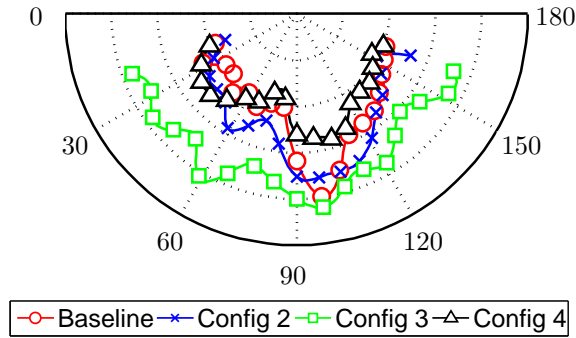

Figure 8. The OASPLA in the microphone array. The interval between the dashed lines crossing the polar axis is $5 dB$.

Table 2. The averaged A-weighted OASPL.

	Baseline	Config. 2	Config. 3	Config. 4
dBA	148.355	149.239	153.582	146.538

Figure 9 displays the comparison of the sound pressure level (SPL) for the configurations. The noise level of the fairing configuration is overall higher than the other configurations. This phenomenon is consistent with the OASPLA shown in Fig. 8. The noise is of broadband type in the frequency range between $100 Hz$ and $5000 Hz$. At the microphones 90° and 100°, an energy bulk is observed at $600 Hz$ for the fairing and reduced bay depth. On the other hand, the baseline configuration exhibits the first characteristic frequency at approximately $700 Hz$ and the secondary one at $1600 Hz$. Moreover, the noise at the microphones of 90° and 100° increases in the frequencies above $1600 Hz$ compared with the other microphones. The increase suggests that the opened door reflects the noise mainly in the frequencies above $1600 Hz$.
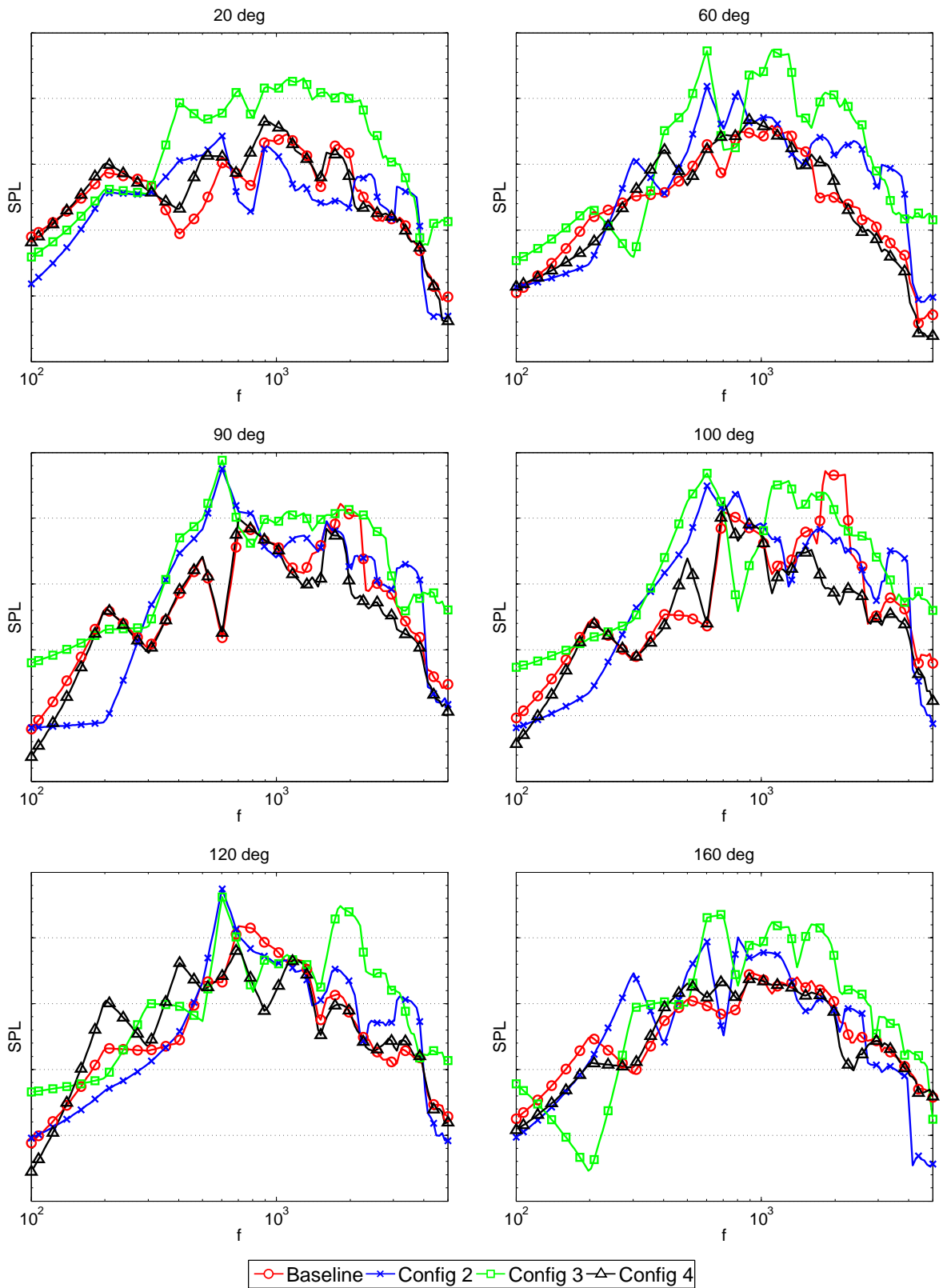
American Institute of Aeronautics and Astronautics

Figure 9. The SPL of the noise at six microphones: 20°, 60°, 90°, 100°, 120°, **and** 160°. **The interval between the major ticks of the Y-axis is** $10dB$.

American Institute of Aeronautics and Astronautics

VI.   Conclusions

Three noise-reduction conceptual designs are investigated for a main landing gear. The configurations are of full scale. The gear door is arranged at an open position to investigate its noise reflection effect. The acoustic computation adopts the SNGR method. This method establishes a procedure on imitating the noise generation and radiation. The turbulent flow that is taken as the noise sources is synthetically constructed using the stochastic model. Thus, the SNGR method cannot provide an assessment as accurate as a CAA method integrated with turbulence-resolved simulation, which can be performed using advanced CFD methods like a hybrid RANS/LES approach. However, the SNGR method gives prediction of the noise on the basis of the statistical quantities of the turbulent flow such as the kinetic energy and specific dissipation rate. The predicted noise level is associated with the energy of the turbulent structures. To a certain extent, the method is moderately accurate for assessment of the statistics of the noise level. Moreover, as the configurations are investigated with the same computational methodology, the results for them should be comparable.

The fairing does not present significant effectiveness on the noise reduction. The bay compressed in the depth is also found ineffective. However, the acoustic liners installed in the bay interior downstream wall can attenuate the noise reflection and further reduce the noise propagating towards the ground. Even though the upstream noise slightly increases due to the acoustic liners, the OASPLA is $1.817 dBA$ lower than the baseline configuration. Moreover, most of reduction is found in the downward arc from 90° to 115°. This region is of interest in industry applications. It is worth noting that all the configurations show a noise increase around the polar angle 100° rather than 90° that corresponds to the normal direction of the opened gear door. The reason is that the wake induced by the wheels and strut contains the majority of the energetic noise sources. The noise at the microphone 100° has higher energy in the frequencies above $1600 Hz$ in comparison with the other microphones. This phenomenon indicates that the gear door mainly reflects the high frequency noise. Therefore, the noise reflection effect of the door is considerable in the case that the horizontally projected area of the door is discernible.

Acknowledgments

References

[1]Crighton, D., "Aeroacoustics of flight vehicles: theory and practice," *NASA Report 1258*, Vol. 1, 1991, pp. 391–447.

[2]Lockard, D. and Lilley, G., "The airframe noise reduction challenge," *NASA/TM-2004-213013*, 2004.

[3]Dobrzynski, W. and H., B., "Full-Scale Noise Testing on Airbus Landing Gears in the German Dutch Wind Tunnel," *AIAA paper 1997-1597*, 1997.

[4]Dobrzynski, W., L., C., Guion, P., and Shiells, D., "A European Study on Landing Gear Airframe Noise Sources," *AIAA paper 2000-1971*, 2000.

[5]Abeysinghe, A., Whitmire, J., Nesthus, D., Moe, J., Vista, C., and Stuczynski, G., "QTD 2 (Quiet Technology Demonstrator) main landing gear noise reduction fairing design and analysis," *AIAA Paper*, Vol. 2007-3456, 2007.

[6]Ravetta, P., Burdisso, R., and Ng, W., "Noise control of landing gears using elastic membrane-based fairings," *AIAA Paper*, Vol. 2007-3466, 2007.

[7]Piet, J.-F., Davy, R., Elias, G., Siller, H., Chow, L., Seror, C., and Laporte, F., "Flight Test Investigation of Add-On Treatments to Reduce Aircraft Airframe Noise," AIAA Paper 20053007, 2005.

[8]Boorsma, K., Zhang, X., Molin, N., and Chow, L. C., "Bluff Body Noise Control Using Perforated Fairings," *AIAA Journal*, Vol. 47, No. 1, 2009, pp. 33–43.

[9]Boorsma, K., Molin, N., and Zhang, X., "Landing gear noise control using perforated fairings," *Acta Mechanica Sinica*, Vol. 26, 2010, pp. 159–174.

[10]Dobrzynski, W., L., C., Guion, P., and Shiells, D., "Experimental Assessment of Low Noise Landing Gear Component Design," *International Journal of Aeroacoustics*, Vol. 9, No. 6, 2010, pp. 763–786.

[11]Smith, M. G., Chow, L. C., and Molin, N., "Control of landing gear noise using meshes," AIAA Paper 2010-3974, 2010.

[12]Murayama, M., Yokokawa, Y., Yamamoto, K., and Hirai, T., "Computational study of low-noise fairings around tire-axle region of a two-wheel main landing gear," *Computers & Fluids*, Vol. 85, 2013, pp. 114–124.

[13]Phillips, B., "Experimental investigation of an acoustic liner with variable cavity depth," NASA TN d-4492, 1968.

[14]Drevon, E., "Measurement methods and devices applied to A380 nacelle double degree-of-freedom acoustic liner development," *10th AIAA/CEAS Aeroacoustics Conference*, AIAA Paper 2004-2907, 2004.

[15]Kabral, R., Bodén, H., and Elnady, T., "Determination of Liner Impedance under High Temperature and Grazing Flow Conditions," AIAA Paper 2014-2956, 2014.

[16]Ma, Z., Smith, M., Richards, S., and Zhang, X., "Attenuation of slat trailing edge noise using acoustic liners," *Aeroacoustics*, Vol. 5(4), 2006, pp. 311–333.

[17]Casalino, D. and Barbarino, M., "Optimization of a Single Slotted Lined Flap for Airframe Noise Reduction," *AIAA Paper*, Vol. 2011-2730, 2011.

[18]Ma, Z. and Zhang, X., "Numerical Investigation of Broadband Slat Noise Attenuation with Acoustic Liner Treatment," *AIAA Journal*, Vol. 47(12), 2009, pp. 2812–2820.

[19]*AIAA Journal*, Vol. 47(12), 2009, pp. 2812–2820.

[20]Lopes, L. V., "Prediction of Landing Gear Noise Reduction and Comparison to Measurements," AIAA Paper 2010-3970, 2010.

[21]W. Béchara, C. Bailly, P. L. and Candel, S., "Stochastic approach to noise modeling for free turbulent flows," *AIAA Journal*, Vol. 32(3), 1994, pp. 455–464.

American Institute of Aeronautics and Astronautics

[22]Bailly, C., Lafon, P., and Candel, S., "Computation of noise generation and propagation for free and confined turbulent flows," *AIAA Paper*, 1996, pp. 1996–1732.

[23]Bailly, C. and Juvé, D., "A stochastic approach to compute subsonic noise using linearized Euler's equations," *AIAA Paper*, 1999, pp. 1999–1872.

[24]M. Billson, L.-E. E. and Davidson, L., "Jet noise modeling using synthetic anisotropic turbulence," *AIAA Paper*, 2004, pp. 2004–3028.

[25]Casalino, D. and Barbarino, M., "A stochastic method for airfoil self-noise computation in frequency-domain," *AIAA Paper*, 2010, pp. 2010–3884.

[26]Kraichnan, R., "Diffusion by a random velocity field," *Physics of Fluids*, Vol. 13(1), 1970, pp. 22–31.

[27]Lighthill, M. J., "On Sound Generated Aerodynamically. I. General Theory," *Proc. Roy. Soc.*, Vol. A 211, 1952, pp. 564–587.

[28]Lighthill, M. J., "On Sound Generated Aerodynamically. II. Turbulence as a Source of Sound," *Proc. Roy. Soc.*, Vol. A 222, 1954, pp. 1–32.

[29]di Francescantonio, P., "A New Kirchhoff Formulation for Transonic Rotor Noise," *Journal of Sound and Vibration*, Vol. 202, No. 4, 1997, pp. 491–509.

[30]Capizzano, F., "Turbulent Wall Model for Immersed Boundary Methods," *AIAA Journal*, Vol. 49(11), 2011, pp. 2367–2381.

[31]Capizzano, F., "Algorithm for the Generation of Euler/RANS Cartesian Grids," *C.I.R.A. Centro Italiano Riecerche Aerospaziali*, Vol. CIRA-cf-07-1121, 2007.

[32]Capizzano, F., "A Compressible Flow Simulation System Based on Cartesian Grids with Anisotropic Refinements," *AIAA Paper*, Vol. 2007-1450, 2007.

[33]He, G.-W., Jin, G. D., and Zhao, X., "Scale-similarity model for Lagrangian time correlations in isotropic and stationary turbulence," *Phys Rrev. E*, Vol. 80, No. 6, 2009, pp. 066313.

[34]Yao, H.-D., Davidson, L., Peng, S.-H., Eriksson, L.-E., and and, M. B., "Determination of Liner Impedance under High Temperature and Grazing Flow Conditions," AIAA Paper 2014-2956, 2015.